2012

System Modeling of Gas Engine Driven Heat Pump

Isaac Mahderekal
shenb@ornl.gov

Bo Shen

Edward A. Vineyard

System Modeling of Gas Engine Driven Heat Pump

Isaac Mahderekal[1]*, Bo Shen[1], Edward A. Vineyard[1]

[1]Building Technologies Research and Integration Center, Oak Ridge National Laboratory
One Bethel Valley Road, P.O. Box 2008, MS-6070
Oak Ridge, TN 37831-6070
Corresponding Author*: Isaac Mahderekal, Email: mahderekali@ornl.gov, Telephone: 1-8655760837

ABSTRACT

To improve the system performance of a gas engine driven heat pump (GHP) system, an analytical modeling and experimental study has been made by using desiccant system in cooling operation (particularly in high humidity operations) and suction line waste heat recovery to augment heating capacity and efficiency. The performance of overall GHP system has been simulated with a detailed vapor compression heat pump system design model. The modeling includes: (1) GHP cycle without any performance improvements (suction liquid heat exchange and heat recovery) as a baseline (both in cooling and heating mode), (2) the GHP cycle in cooling mode with desiccant system regenerated by waste heat from engine incorporated, (3) GHP cycle in heating mode with heat recovery (recovered heat from engine). According to the system modeling results, by using the desiccant system the sensible heat ratio (SHR- sensible heat ratio) can be lowered to 40%. The waste heat of the gas engine can boost the space heating efficiency by 25% at rated operating conditions.

1. INTRODUCTION

Recently, the Gas Engine-Driven Heat Pump (GHP) System has become an economic choice and more attractive climate control system than the conventional air conditioner due to its advantage in reducing fossil fuel consumption and environmental pollution. The GHP is a new type of heat pump in which the compressor (the core part) is driven by a gas engine. The GHP typically uses the work produced by the engine to drive a vapor-compression heat pump. At the same time, the waste heat rejected by the engine is used to augment the heating capacity of the GHP.

Generally, fuel is mainly converted to electrical energy at power plants and the waste heat is discharged to the environment, then electrical energy is transmitted to Electric heat pumps (EHPs) and is converted to mechanical energy by the motor of the EHPs. In this process, energy is converted twice and the heat loss is high as shown in Figure 1.

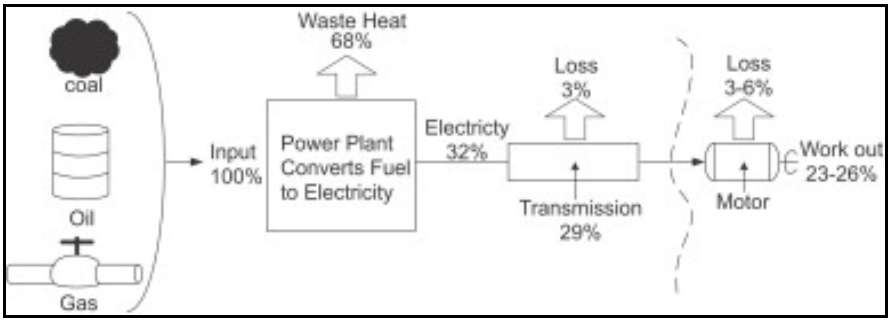

Figure 1: Transmission from Source Energy to Electric Heat Pumps

However, energy efficiency can become higher if fuel conversion can be located closer to where heat is required. Then the heat released in the conversion can be more efficiently used. GHPs are harmonious with this concept as they have high energy efficiency, especially in heating.

Much is expected from GHPs as a product that would help satisfy the air conditioning system demand from medium and small sized buildings while reducing electric utility peak power demand in summer and saving energy in

general. A GHP can be a more attractive climate control system than the conventional heat pumps for a number of reasons, e.g.:

A. Variable speed operation: Typically, the GHP can cycle at minimum speed and modulate between a minimum and maximum speed to match the required load. The minimum and maximum speeds are decided by the performance of the engine and compressor. As a result, the part load efficiency of such a system will be high. Its seasonal operational cost and cycling losses will be lower than those of a single speed system with an on–off control system.

B. Engine heat recovery: The engine's heat efficiency is not very high (about 30% for gas engines now). The heat of fuel combustion is wasted through exhaust gases, cooling water and the engine block. However, the GHP system's efficiency will be increased by recovering the heat from the cooling water and the exhaust gases.

C. Natural gas fuel: GHPs also differs from electric heat pumps (EHP) in the energy they use, primarily natural gas or propane instead of electricity. So, a GHP is preferred in a region where electric costs are high and natural gas is readily available.

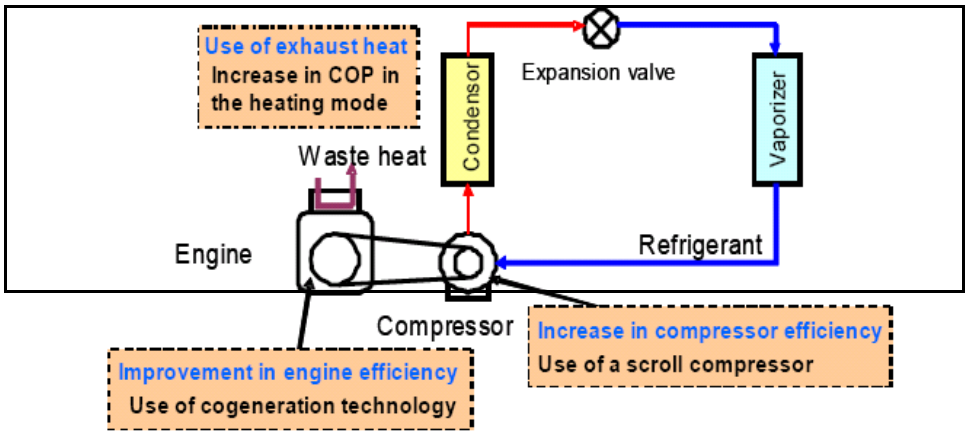

Figure 2: Basic Diagram of a GHP

As shown in Figure 2, the GHP typically uses the work produced by the engine to drive a vapor-compression heat pump. At the same time, the waste heat rejected by the engine is used for heating purposes. Thus, the GHP is inherently more efficient than conventional heating-systems currently marketed (e.g. furnace, direct-fired absorption heat-pump or electrical heat pump). Since the high energy efficiency of GHPs causes low fossil fuel consumption, the environmental pollution could be reduced. In addition the energy sources used for GHPs, such as natural gas, propane or liquefied petroleum gas (LPG), can be less expensive than electricity in many locales, so GHPs become an economic choice. Furthermore, GHPs can play important social and economic roles by effectively balancing electricity demand, mitigating the electricity peaks and adjusting the energy configuration.

2. DESCRIPTION OF A GHP

A heat pump is used to transfer thermal energy from a low temperature reservoir to a high temperature field to cool or heat. The GHP is a new type of heat pump in which the compressor (the core part) is driven by a gas engine. In this study the GHP system shown in Figure 3 will be investigated. The GHP system consists of the gas engine (E-1), an open type compressor (K1-A and B), pump (P-1), thermostatic expansion valve (TXV), oil separator (S-2), outdoor heat exchanger (C-1), indoor heat exchanger (C-2A), radiator (C-3), coolant exhaust heat exchanger (EAX-1) and valves. In addition to these common components of a regular GHP, this study will also investigate adding a heat recovery heat exchanger (HEX) to improve the performance of the GHP in cooling and heating mode respectively. Specifications of the GHP used for this study are summarized in Table 1.

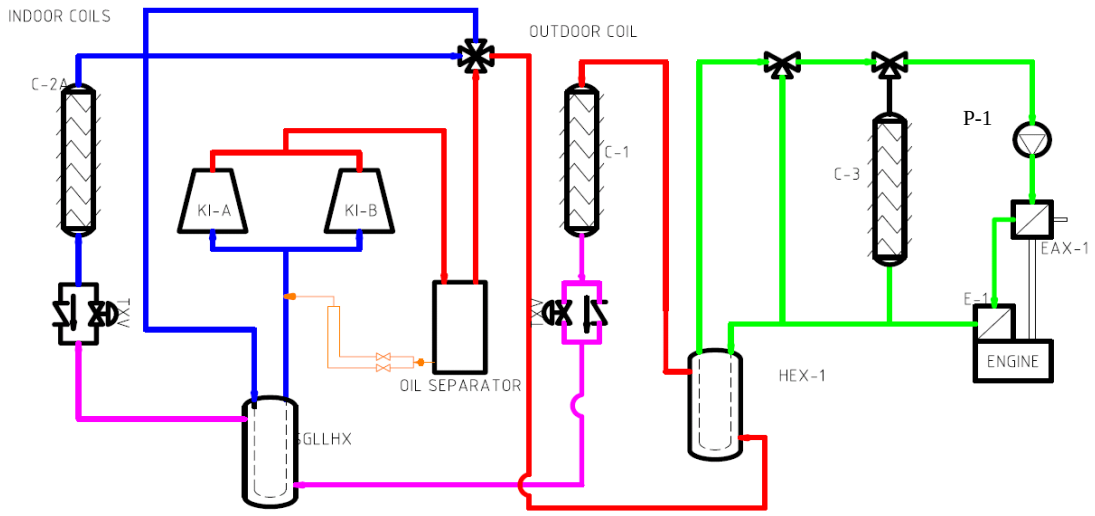

Figure 3: Schematic Diagram of GHP to be Studied

During both heating and cooling operation, engine coolant is circulated throughout the system by a coolant pump. Warm coolant is pumped through the exhaust heat exchanger (shell and tube heat exchanger), where its temperature is raised a few degrees by waste heat recovered from the engine exhaust. The coolant then flows to the water cooled exhaust manifold located on the internal combustion engine, where its temperature is further increased. The coolant then enters the internal combustion engine and removes heat from the engine. This portion of the coolant circuit is where engine waste heat is recovered for efficient use during the heating or cooling cycle. When the GHP is operated in the heating mode, waste heat is removed from the engine and exhaust by the coolant and is directed to the HEX, thus transferring part of the recoverable waste heat from the engine into the suction stream of the refrigerant cycle. When the GHP is operated in the cooling mode, waste heat is removed from the engine and exhaust by the coolant directed to an air-to-coolant heat exchanger (not shown in Figure 3) to heat the outdoor air stream. The heated outdoor air stream regenerates a desiccant wheel, which processes the indoor return air stream, in order to reduce its humidity. The remaining engine heat is directed to the radiator and rejected to the atmosphere.

Table 1: GHP Specifications

Engine	Water-cooled, 4 cycle, 3 cylinder, 9.5kW rated output
Engine speed	1200 to 2450 rpm
Fuel type	Natural gas or propane
Compressor	Scroll type, 60.5 $\frac{cm^3}{hr}$
Compressor	2280 to 4655 rpm
Refrigerant type	R410A
Design cooling rating	120,000 $\frac{Btu}{hr}$
Design heating rating	140,000 $\frac{Btu}{hr}$
Electrical power requirement	2 kW

3. MODEL DESCRIPTIONS

Mass flow rate and power calorimeter test data for scroll compressors have been collected. These test data are commonly correlated with 10-coefficient polynomials using the method presented in ARI Standard 540 as a function of the saturated evaporator and condenser temperatures. In general, these polynomial representations accurately represent the experimental data. Twenty-one sets of calorimeter test data have been collected on compressors using R-410A (CH_2F_2/CHF_2CF_3) as the refrigerant. The compressors were tested at seventeen different operating conditions (different saturated evaporating and condensing temperatures). The condensing temperatures ranged from 90°F (32.2°C) to 140°F (60°C) and the evaporating temperature ranged from 1.5°F (-16.9°C) to 53°F(11.7°C). For each evaporating and condensing condition, experimental values of power input and refrigerant mass flow rate given. ARI Standard 540 uses a bivariate cubic polynomial with cross-terms (Equation (1)) to describe the mass flow rate and the power input as a function of saturated evaporating and condensing temperatures with a standard compressor suction superheat of 20°F (11.1 K). The compressor speed ranges from 2300 to 4600 RPM. The polynomial coefficients at 2380 RPM and 3400 RPM, for mass flow and power are summarized in Table 2.

$$F(S,D) = \lambda_1 + \lambda_2 S + \lambda_3 D + \lambda_4 S^2 + \lambda_5 DS + \lambda_6 D^2 + \lambda_7 S^3 + \lambda_8 DS^2 + \lambda_9 SD^2 + \lambda_{10} D^3 \quad (1)$$

Where:

$\lambda_1 - \lambda_{10}$ are the map coefficients per ARI Standard 540,

S & D are the compressor suction & discharge saturation temperatures (°F)

Table 2: The Ten Coefficients Based on the Polynomial Fit

Compressor Speed				
	2380 rpm		**3400 rpm**	
Mass flow and power	$\dot{m}_{map}$	$\dot{W}_{map}$	$\dot{m}_{map}$	$\dot{W}_{map}$
	[$\frac{lbm}{hr}$]	[W]	[$\frac{lbm}{hr}$]	[W]
λ_1	3.48E+02	6.18E+02	5.07E+02	5.70E+02
λ_2	2.26E+00	-8.86E+00	3.39E+00	-1.07E+01
λ_3	-3.52E+00	-8.44E+00	-4.93E+00	-3.67E+00
λ_4	5.63E-02	2.86E-01	8.44E-02	3.50E-01
λ_5	4.41E-02	1.04E-01	6.56E-02	1.44E-01
λ_6	3.56E-02	2.85E-01	5.05E-02	3.43E-01
λ_7	-2.16E-04	-2.24E-03	-3.19E-04	-3.09E-03
λ_8	-1.08E-05	-2.10E-03	-1.96E-05	-2.66E-03
λ_9	-1.93E-04	3.53E-06	-2.86E-04	-5.16E-05
λ_{10}	-1.17E-04	-5.97E-04	-1.67E-04	-6.63E-04

The engine used for the GHP application is shown in Figure 4. This 3-cylinder water-cooled engine featuring high torque in the low rpm range is designed to run on natural gas and LPG (propane)/CNG (compressed natural gas).

Figure 4: Engine Compressor Sub-Assembly

The engine oil sump contains 35 liters of oil. This excess oil allows a maintenance interval of every 6,000 hours and total engine life of 40,000 hours. Summary of engine specifications is shown in Table 3:

Table 3: Engine Specification

Item	Description
Model	950P
Type	4-stroke, Water cooled
Cylinder number	3
Displacement	950 cm^3
Compression ratio	9.3
Rated output	9.5 kW
Revolution range	1000 to 2800 rpm
Thermal efficiency	29 % (HHV) at maximum engine output
Enclosing oil amount	35 L
Maintenance interval	Every 6,000 hours
Engine life	40,000 hours

The thermodynamic model of the engine is obtained by the means of experiment from the manufacturer. The steady working condition of the engine is mainly a function of load and speed. In this system modeling, the concerned parameters are engine power output, fuel flow rate (fuel input) and recoverable waste heat. Engine test data has been used to get the relationship between the engine thermodynamic parameters in a wide range of loads and speeds, as shown in Equation (2) a second order bivariate regression polynomial equation.

$$y = \lambda_1 + \lambda_2 n + \lambda_3 n^2 + \lambda_4 T_r + \lambda_5 T_r^2 + \lambda_6 n T_r + \lambda_7 n T_r^2 + \lambda_8 n^2 T_r + \lambda_9 n^2 T_r^2 \quad (2)$$

Where output *y* represents the power output, fuel input and recoverable engine heat, n represents engine speed and T_r represents torque. Engine testing produced 66 valid data points with the engine speed ranging from 1000 to 2800 rpm (the engine speed has a constant ratio of 0.59 to the compressor speed), and torque ranging from 10 to 45 lbf-ft (13.6 to 61.0 N-m). The constants of the polynomials are shown in Table 4.

Table 4: Constants of Polynomial for Equation (2)

	Fuel Flow rate	Engine Efficiency	Available Heat for Recovery
	[$\frac{ft^3}{hr}$]	[dimensionless]	[$\frac{Btu}{hr}$]
λ_1	-26.47329569	0.146090488	-21344.09465
λ_2	0.061083092	-0.000145029	49.24824295

λ_3	-1.30634E-05	4.61466E-08	-0.010532395
λ_4	2.359119883	0.007313038	1902.040406
λ_5	-0.028564226	-0.000112128	-23.02990683
λ_6	-0.003316893	1.33269E-05	-3.037913267
λ_7	5.92833E-05	-1.68974E-07	0.04779719
λ_8	1.13882E-06	-4.15607E-09	0.000918174
λ_9	-1.57016E-08	5.58081E-11	-1.26594E-05

We modeled the Fin-&-Tube evaporator and condenser using segment-by-segment approach. Each tube segment has individual air side and refrigerant side entering states, and considers possible phase transition. The coil model can simulate arbitrary tube, fin geometries and circuitries, any refrigerant side entering and exit states, misdistribution, and accept two-dimensional air side temperature, humidity and velocity local inputs. The tube circuitry and 2-dimensional boundary conditions are provided by an input file. In addition to the functionalities of the segment-to-segment fin-tube condenser, the evaporator model is capable of simulating dehumidification process. In the studies below, we simulated the indoor and outdoor air-to-refrigerant heat exchangers using their actual geometry and configuration as inputs to the heat pump system model.

The desiccant modeling uses heat & mass analogy method to simulate process side and regeneration side energy transfer based on given effectiveness. The effectiveness input to the model is based on the manufacturer's data. The model can simulate any entering air temperature and humidity levels, and predict temperature and humidity change at the process side and the regeneration side. This is the same model used in TRNSYS (Klein 2010).

For the suction line heat recovery (refrigerant-to-coolant) and the air-to-coolant (upstream of desiccant wheel) heat exchangers, we adopted a simple effectiveness method, which specifies a heat transfer effectiveness directly. Both the indoor blower and the outdoor fan are single-speed, electricity-driven. The indoor blower drives the air flow rate of 4000 CFM, with 1000 Watts power consumption, and the outdoor fan drives 8000 CFM, using 750 Watts.

4. COOLING PERFORMANCE

In cooling mode, the recovered engine heat is utilized to heat up an outdoor air stream in an air-to-coolant coil, which has a heat transfer effectiveness of 0.5 (air stream has the smaller specific heat flow rate). The heated outdoor air stream regenerates a desiccant wheel. Indoor return air flows through the process side of the desiccant wheel. Flow rates for the regeneration and indoor air streams are selected to be the same. Regarding the desiccant wheel, the process effectiveness is fixed at 0.1 and the regeneration effectiveness is 0.7, representative of a low performance wheel. The effectiveness values were obtained from Panaras et al. (2010). The compressor superheat degree and the condenser subcooling degree are specified at 10 °R. It is assumed there are no line heat and pressure losses, since this is a packaged unit and the lines are short. The compressor shell heat loss is fixed at 10% of the compressor power consumption at various conditions.

We conducted a parametric study by varying the compressor speed from 2300 RPM to 4600 RPM, and varying the entering water temperature (EWT) to the heat recovery air-to-coolant coil from 100 °F to 130 °F. The operational condition is selected as outdoor air dry bulb temperature at 95 °F, indoor (return air) dry bulb temperature at 80 °F, and indoor wet bulb temperature at 67 °F. The outdoor specific humidity is the same as the indoor humidity. For calculating the air side total cooling capacity and sensible heat transfer ratio, we consider difference between the return air to the desiccant wheel and the air exiting the indoor air-to-refrigerant coil.

The equivalent electricity EERsbased on, net cooling capacity (total cooling capacity minus indoor blower power) divided by the sum of the compressor indoor blower and outdoor fan power, are shown in Figure 5. The source energy COPs are shown in Figure 6, which is obtained using the net cooling capacity divided by the engine energy input rate, plus the equivalent source energy rates for the blower and fan. We use a conversion factor of 0.32 to

convert source energy consumption to electricity consumptions. Figure 5 and Figure 6 illustrate that magnitude of the recovered heat flow rate, i.e. the entering water temperature to the heat recovery air-to-coolant coil, doesn't impact the efficiency noticeably. The major influential factor on the site and the source efficiencies is the compressor speed. The efficiencies increase as compressor speed drops.

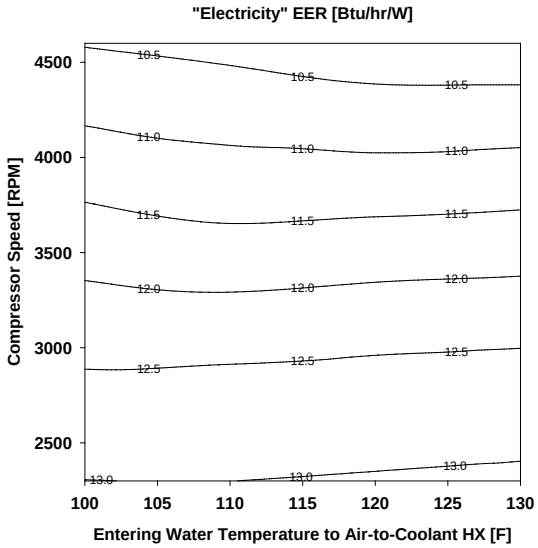

Figure 5: Equivalent "Electricity" EER vs. EWT and compressor speed in cooling mode

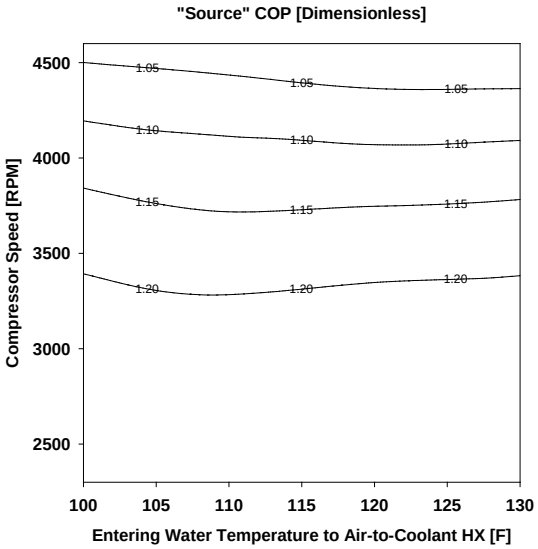

Figure 6: "Source" efficiency vs. EWT and compressor speed in cooling mode

Figure 7 and Figure 8 show the total cooling capacity and the sensible heat ratio, varying with the compressor speed and EWT. One can see that the total cooling capacity is mainly a function of the compressor speed. However, the EWT has a significant impact on the sensible heat ratio (SHR) - SHR decreases with increasing EWT. This means that the total cooling capacity is relatively constant at each compressor speed, but allocation of the sensible cooling and latent cooling capacity is determined by the EWT. The modeling also revealed that the SHR increases with the compressor speed at a constant EWT. This is contrary to a regular variable-speed vapor compression system without using a desiccant-wheel, where SHR is always reduced by increasing the compressor speed at a constant indoor air flow rate. The explanation is, for the desiccant-wheel coupled GHP, the latent load is totally removed by the desiccant wheel, and thus, elevating the compressor speed only results in a larger sensible capacity.

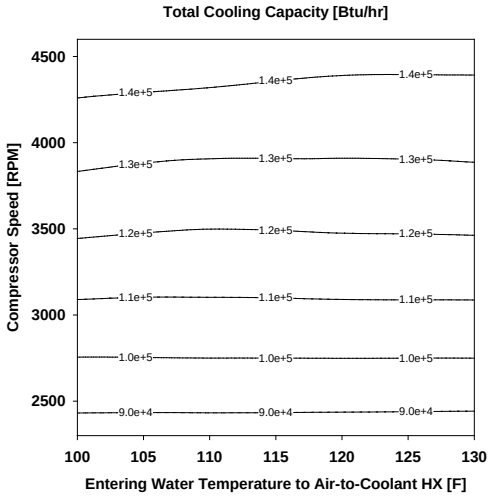

Figure 7: Total cooling capacity vs. EWT and compressor speed in cooling mode

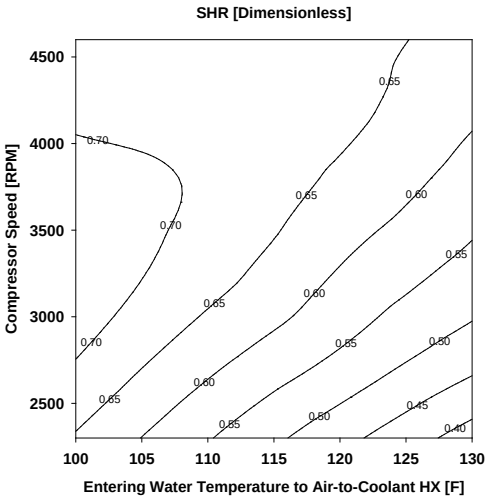

Figure 8: SHR vs. EWT and compressor speed in cooling mode

Table 5 shows comparisons of performance indices, between the desiccant-wheel coupled GHP at EWT of 130 °F and the baseline GHP without the heat recovery. The desiccant-wheel coupled GHP significantly enhances the dehumidification capability, without changing the total cooling capacity. However, it should be noted that using the desiccant-wheel to remove the indoor latent load is at the expense of introducing extra sensible load to the conditioned space. The drawback in utilizing the desiccant wheel is a decrease in EERs compared to the baseline GHP. If the added fan and pump power used by the air-to-coolant coil and the desiccant wheel are taken into account, the efficiency degradation is even larger. Thus, the desiccant-wheel coupled GHP should be used only in applications where humidity removal needs are paramount.

Table 5: Comparisons between GHP with or without using desiccant-wheel

Compressor Speed [RPM]	EER with heat recovery $[\frac{Btu}{hr}{W}]$	EER without heat recovery $[\frac{Btu}{hr}{W}]$	Total Capacity with heat recovery $[\frac{Btu}{hr}]$	Total Capacity without heat recovery $[\frac{Btu}{hr}]$	SHR with heat recovery	SHR without heat recovery
2300	13.1	13.1	85265	86981	0.38	0.85
2800	12.7	12.8	101575	103591	0.47	0.80
3300	12.1	12.4	115797	118612	0.54	0.76
3800	11.4	11.8	128083	132235	0.58	0.73
4300	10.6	11.1	138276	144285	0.62	0.71
4600	10.2	10.7	143715	150916	0.63	0.70

5. HEATING PERFORMANCE

In heating mode, recovered engine heat is used to heat up the refrigerant vapor in the suction line in a refrigerant-to-coolant heat exchanger. The heat transfer effectiveness of the suction line heat exchanger is fixed at 0.5 (refrigerant vapor stream has the smaller specific heat flow rate). The outdoor evaporator exit is saturated vapor, since it is connected with a suction line accumulator, and the indoor condenser subcooling degree is fixed at 10 °R. The compressor shell heat loss ratio is assumed to be 30%. The water temperature entering the suction line heat exchanger is controlled at 200 °F, which seeks a maximum heat recovery without boiling the water.

It should be noted that the suction line heat exchanger, using the recovered engine heat, can greatly elevate the superheat degree, consequently, the vapor density at the compressor suction port and the mass flow rate decrease. Thus the compressor map predictions (Equation (1)) must be corrected for variation in the suction superheat, as compared to the standard superheat degree of 20 °F. The method of Dabiri and Rice (1981) was adopted to correct the mass flow rate calculation, as given in Equation (3).

$$\dot{m}_{ref,actual} = [1 + F_{mass}(\frac{v_{ARI-map}}{v_{act}} - 1)]\dot{m}_{ref,ARI-map} \quad (3)$$

where F_{mass} is an empirical correction factor assigned a value of 0.75, $\dot{m}_{ref,ARI-map}$ and $\dot{m}_{ref,actual}$ are the mass flow rates at the standard (compressor map) and actual suction superheat, and $v_{ARI-map}$ and v_{act} are the specific volumes at the standard and actual superheat. For the compressor power adjustment, we adopted the same multiplier as the mass flow rate correction, based on the assumption that the isentropic efficiency and the polytropic exponent are insensitive to the variation of the suction superheat degree.

We ran a two dimensional parametric study by varying the compressor speed from 2300 RPM to 4600 RPM, at three ambient temperatures of 17 °F (72% RH), 32 °F (70% RH) and 47 °F (68% RH). Figure 9 shows the equivalent "electric" COP as a function of the compressor speed and ambient temperature – COP based on total heating capacity (condenser heat plus indoor blower heat) divided by the sum of the compressor, indoor blower and outdoor fan power. We can see that the EER has a strong dependence on the ambient temperature, and slightly increases as the compressor speed drops. Figure 10 shows variation of the vapor temperature at the compressor suction port, which ranges from 100 F to 120 F. The modeling has shown that a fraction of the available waste heat is recovered by the refrigerant. Figure 11 shows the actual "source" COPs using the suction line heat exchanger for heat recovery. It is encouraging to see that the "source" COP can be larger than 1.0 at the low ambient temperature of 17 °F. Figure 12 demonstrates the maximum possible "source" COPs, assuming the remaining engine waste heat is

totally recovered by an air-to-coolant coil downstream of the indoor air-to-refrigerant coil. Comparing Figure 11 to Figure 12, we can see that further utilization of the engine waste heat can boost the "source" COP up to 20%.

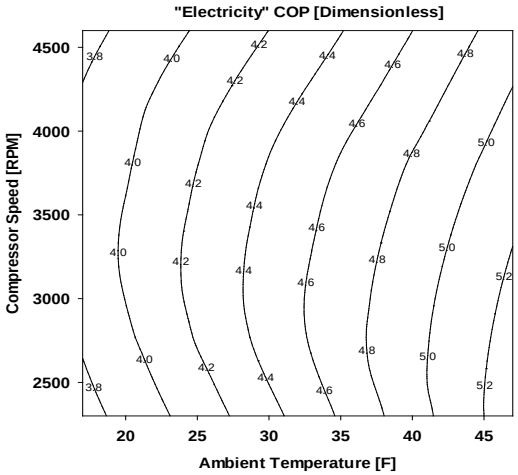

Figure 9: Equivalent "electric" COP vs. ambient temperature and compressor speed in heating mode

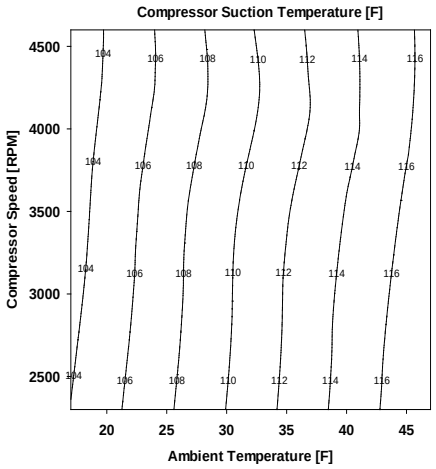

Figure 10: Compressor suction temperature vs. ambient temperature and compressor speed in heating mode

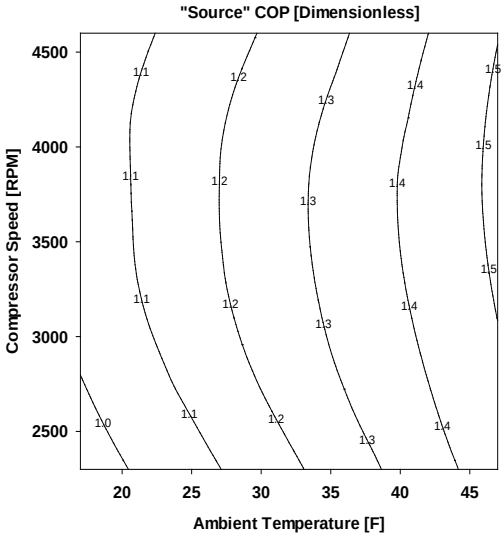

Figure 11: "Source" COP vs. ambient temperature and compressor speed in heating mode

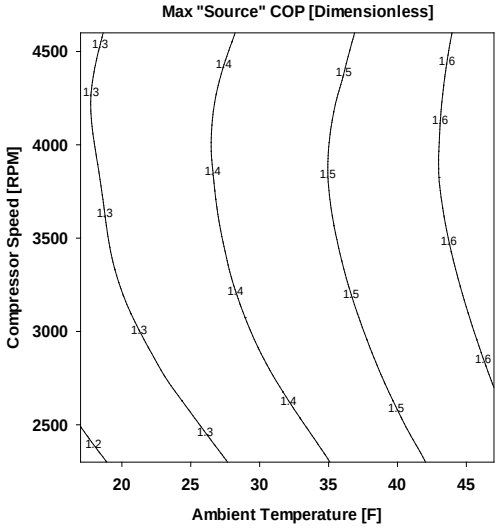

Figure 12: Max "Source" COP vs. ambient temperature and compressor speed in heating mode

Figure 13 and Figure 14 show comparisons between the GHP with and without suction line heat recovery. We can see that using the suction line heat recovery can increase the heating COPs by 16% to 25%. However, it doesn't boost the heating capacity to the same degree. As discussed above, using the suction heat recovery reduces the suction vapor density, and thus, decreases the compressor mass flow rate and power consumption. The added capacity by the suction heating and the lost capacity due to the decreased compressor indices offset each other.

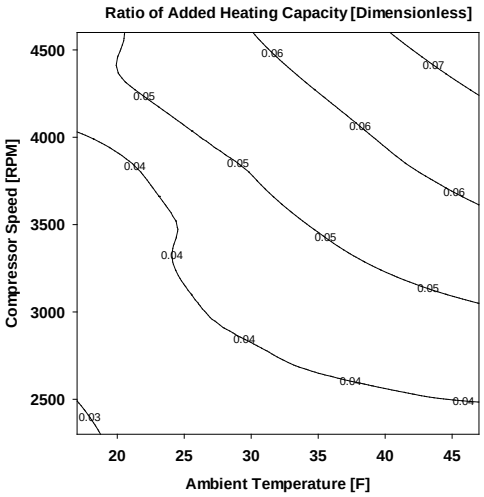

Figure 13: Ratio of added heating capacity due to suction line heat recovery vs. ambient temperature and compressor speed in heating mode

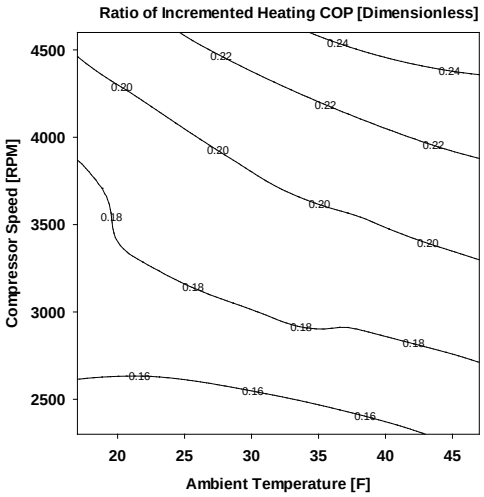

Figure 14: Ratio of incremented COP due to suction line heat recovery vs. ambient temperature and compressor speed in heating mode

6. SUMMARY

Gas engine driven heat pumps (GHP) can operate with high source energy efficiency, due to their variable-speed capability utilization engine heat recovery. Using suction line heat recovery can boost the capacity and efficiency in heating mode. A desiccant-wheel coupled GHP, regenerated by the engine waste heat, can significantly augment the dehumidification capacity of a GHP making it attractivefor applications with high humidity conditions.

The means of heat recovery used in this study can't recover all the engine waste heat. To further improve the source energy efficiency, we might add an indoor air-to-coolant heat recovery coil for heating mode, or use the remaining waste heat for domestic water heating.

REFERENCES

ANSI/ARI Standard 540-99, 1999, "Positive Displacement Refrigerant Compressors and Compressor Units", Air-Conditioning and Refrigeration Institute, Arlington, VA

Dabiri, A. E. and C.K. Rice, 1981. "A Compressor Simulation Model with Corrections for the Level of Suction Gas Superheat," *ASHRAE Transactions*, Vol. 87, Part 2, pp.771-782.

Panaras, S., E. Mathioulakis, V. Belessiotis, N. Kyriakis, 2010, "Experimental validation of a simplified approach for a desiccant wheel model", *Energy and Building*, Vol. 42, pp. 1719-1725.

S. A, Klein. 2010, "TRNSYS 16.0 User Manual".

Z. Lian, S. Park, W. Huang, Y. Baik and Y. Yao, Conception of combination of gas-engine-driven heat pump and water-loop heat pump system, *Int J Refrigeration* 28 (2005), pp. 810–819